Available online at website: https://journal.bcrec.id/index.php/bcrec

Bulletin of Chemical Reaction Engineering & Catalysis, 20 (4) 2025, 661-671

Original Research Article

Design of Bi-and Tri-metal Oxide Photocatalysts via Gelatin-Directed Mesoporous Silica Hard Templating for Advanced Dye Degradation

Maria Ulfa*, Suwiji Lestari

Chemistry Education Study Program, Faculty of Teacher Training and Education, Sebelas Maret University, Jl. Ir. Sutami 36A, Surakarta 57126, Indonesia.

Received: 1st August 2025; Revised: 21th September 2025; Accepted: 22th September 2025
Available online: 27th September 2025; Published regularly: December 2025

Abstract

This study aims to develop a photocatalyst combination of NiO, CuO and ZnO metal oxides modified with mesoporous silica gelatin (mSG) to overcome methylene blue (MB) dye waste through photodegradation process. The photocatalysts were synthesized using the hard template method with mSG as the matrix and tested for their performance towards MB degradation under ultraviolet light. Characterization results showed that the G-Ni-Cu-Zn photocatalyst has a larger surface area, better crystalline structure, nano particle size (~26 nm), and band gap energy of 3.16 eV compared to G-Ni-Zn which has a very low surface area, larger particle morphology (~0.46 µm), and band gap energy of 2.13 eV. Photodegradation tests showed a maximum degradation efficiency of 83.67% by G-Ni-Cu-Zn in 120 minutes, which is much higher than that of G-Ni-Zn.

Keywords: photocatalyst; mesoporous silica; hard template; characterization; methylene blue

How to Cite: Ulfa, M., Lestari, S. (2025). Design of Bi-and Tri-metal Oxide Photocatalysts via Gelatin-Directed Mesoporous Silica Hard Templating for Advanced Dye Degradation. *Bulletin of Chemical Reaction Engineering & Catalysis*, 20 (4), 661-671. (doi: 10.9767/bcrec.20460)

Permalink/DOI: https://doi.org/10.9767/bcrec.20460

1. Introduction

The rapid development of Indonesia's textile industry, accelerated by the Making Indonesia 4.0 initiative, has generated substantial environmental challenges, particularly from textile dye waste [1-3]. Approximately 92 million tons of textile waste are produced annually, with methylene blue (MB) being a prominent synthetic dye pollutant [4]. Methylene Blue ($C_{16}H_{18}ClN_3S$) is a cationic heterocyclic aromatic compound that is highly resistant to natural degradation and poses significant environmental and health risks, including carcinogenicity and aquatic ecosystem damage [5-7]. Methylene Blue is used as a dye in silk, wool and cotton fabrics and other textile materials. Methylene Blue can also damage aquatic ecosystems. Although there is no universally accepted international guideline that specifies an allowable concentration of methylene blue in water, methods established by US EPA for methylene blue active substances (MBAS) enable detection down to ~ 0.025 mg/L in water. This low detection limit underscores the potential for environmental impact even at low concentrations. Regulatory thresholds vary by country and region, often much lower than local ministerial standards, to protect aquatic life and human health [8].

Conventional treatment methods such as adsorption, ozonation, and electrocoagulation have limitations, particularly in completely decomposing complex dye compounds rather than merely transferring them to another phase [9,10].

* Corresponding Author.
Email: mariaulfa@staff.uns.ac.id (M. Ulfa)

Methods, such as adsorption, have a simple process, but often cause new problems, namely the production of new phases of more concentrated pollutants because they only transfer dyes from the liquid phase to the solid phase, not decomposing the complex compounds of these dyes [11].

The right alternative in minimizing this problem is by using the principle of photodegradation using semiconductors and ultraviolet light. Photodegradation is a process of decomposing an organic compound with the help of photon energy. The principle of photodegradation is that if photon energy hits a metal semiconductor, electrons jump from the valence band to the conduction band [12]. This process requires a photocatalyst which is generally a semiconductor material, such as: TiO_2, ZnO and Al_2O_3. Photocatalyst activity will increase with the absorption of UV light, resulting in electrons and holes (e^-, h^+) [13]. Hole is a positive hole caused by the displacement of electrons. Electrons and holes are important species to start the photodegradation process [14].

In previous research, the photodegradation process has been carried out with several semiconductor materials, including research on the photodegradation of methylene blue using ZnO-AC photocatalysts, the use of semiconductor photocatalysts has several advantages including being able to carry out total mineralization of organic pollutants, low cost, relatively fast process, non-toxic, and has the ability to be used in the long term [15]. Based on research on the photodegradation of methylene blue and congo red with ZnO NPs photocatalyst produced a degradation percentage of 91.81% [16]. While research on photodegradation of methylene blue with Cu-doped TiO_2 catalyst produced a dye presentation of 75.9% [17].

In the photodegradation process the amount of catalyst added can increase the photocatalysis reaction, if added in excess it reduces the activity of the catalyst in forming hydroxy radicals. Increasing radiation time in the photodegradation process can increase the amount of degraded dyes, the results of this process are CO_2, H_2O and mineral acids [18]. Based on this description, research was carried out on the photodegradation process of methylene blue with NiO-CuO-ZnO combination photocatalysts at various concentration variations. Nickel (Ni) in the form of NiO oxide has characteristics that can increase acidity and increase the adsorption ability of photocatalysts [19]. Copper oxide (CuO) is used to improve photocatalyst performance because it can expand the absorption of light into the visible region [20]. Zinc oxide (ZnO) is commonly used as a catalyst in the form of ZnO, due to its chemical stability and high catalytic activity [20].

Metal oxide photocatalysts can be used in the methylene blue photodegradation process because they have the ability to increase the efficiency of the catalytic process. The combination of two metals (bimetal) is expected to produce more catalytic cycles, enhance the interaction with light, and facilitate the series of reactions required to degrade methylene blue more effectively. However, if the photocatalyst synthesis is carried out at high temperatures, the NiO-CuO-ZnO particles clumps together, forming larger particles and reducing the surface area of the photocatalyst so that the photocatalytic activity decreases [21]. Therefore, a material is needed to increase the photocatalytic activity of NiO-CuO, CuO-ZnO and NiO-ZnO metal oxide combinations. Mesoporous silica is the best type of silica to increase the photocatalytic activity of Ni-Cu-Zn, because it has a large enough surface area, so it can accommodate more Ni-Cu-Zn photocatalysts, besides high stability and can be used for a long time [22].

One source that can be used as a mesoporous silica material is gelatin. Gelatin is an environmentally friendly pore structuring agent. The addition of gelatin is needed to provide good mechanical properties and structural strength [23]. The mesoporous silica formed can then be used as a template in the hard template method in the synthesis of photocatalyst materials. The hard template method itself has optimal template resistance to high temperatures and has better control over the size and morphology of the material, which distinguishes it from the soft template method [24].

Therefore, there is a need for a solution in the treatment of methylene blue dye waste through the photodegradation method with Ni-Cu-Zn metal combination photocatalysts with increased photocatalytic activity through the use of gelatin mesoporous silica material. In addition, the combination of metals is easily obtained at an economical price, and provides a positive effect that cannot be provided by one metal, so in this research using a combination of Cu-Ni; Cu-Zn and Ni-Zn metals as photocatalyst materials with mesoporous silica from high gelatin processed through the hard template method to degrade methylene blue textile dye waste.

2. Materials and Method

2.1 Materials

The materials used in this study are HCl 37% (MW = 36.5 g/mol), $Ni(NO_3)_2.6H_2O$ 98% (MW = 229.54 g/mol), $CuCl_2.2H_2O$ 99% (MW = 170.49 g/mol), $Zn(NO_3)_2.6H_2O$ 99% (MW = 297.48 g/mol), commercial gelatin (MW = 90.00 g/mol), distilled water (MW = 18 g/mol), triblock copolymer pluronic P123 (MW = 5750 g/mol), Tetraethyl

Orthosilicate (TEOS) 99% (MW = 208.33 g/mol), Methylene Blue (MW = 319.85 g/mol), $C_6H_8O_7.H_2O$ 99% (MW = 192.12 g/mol), NaOH 99% 1 M (MW = 39.99 g/mol), plastic wrap.

2.2 Synthesis of Mesoporous Silica using Gelatin (mSG)

Mesoporous silica modified with gelatin (mSG) was synthesized via a sol–gel self-assembly method. A total of 4 g of P123 and 0.8 g of gelatin were weighed using an analytical balance, then HCl solution was made by diluting 19.5 mL of 37% HCl in 127 mL of distilled water. The mixture of P123 and gelatin was stirred at 40 °C using a stirrer at 500 rpm for 3 hours under plastic wrap, while continuously dripping the HCl solution using a burette. After that, 242.08 mL of TEOS was added to the mixture, then the stirring process was continued under the same temperature and speed conditions for 24 hours. The formed mixture was then put into an autoclave hydrothermal reactor and heated in an oven at 90 °C for 24 hours in a closed bottle (aging process). The heating results were filtered using filter paper and Buchner funnel, then the white precipitate obtained was washed with 200 mL of distilled water and filtered again using Buchner funnel. The filtered precipitate was then heated in an oven at 70 °C for 24 hours, followed by reheating at 100 °C for 24 hours. The final stage is the calcination process carried out in a furnace at 550 °C for 5 hours until SPG-20 powder is obtained.

2.3 Activation and Sulfonation of mSG

The mSG was acid-activated by immersion in 0.05 L of 0.1 M HCl for 24 h. After filtration and rinsing with deionized water, the solid was dried at 90 °C. Sulfonation was performed by refluxing 1 g of mSG with 0.01 L of concentrated H_2SO_4 at 90°C for 20 h under stirring in a three-neck flask equipped with a reflux condenser. The resulting sulfonated material (denoted as sulfonated mSG) was filtered, thoroughly washed with hot deionized water, and dried at 90 °C. Additional batches with varying acid volumes (0.001 L and 0.005 L) were prepared to examine the degree of sulfonation.

2.4 Impregnation of Metal Oxides into Sulfonated mSG

A total of 1.25 g of SPG-20 was taken as a mesoporous silica hard template. The $Ni(NO_3)_2$-$6H_2O$ compound was dissolved in 10 mL of deionized water, and the same steps were taken to dissolve the $Zn(NO_3)_2$-$6H_2O$ compound. The two solutions were then mixed and stirred until homogeneous to form a Ni-Zn mixture, then stirred for 1 hour. The mixture was then put into the SPG-20 precursor and stirred again until evenly mixed. Next, 5 mL of $C_6H_8O_7$-H_2O catalyst was added dropwise to the mixture to accelerate the reaction, then stirred for 1 hour at 70 °C to evaporate the water. The mixture that has been formed is then dried at 100 °C for 24 hours, followed by heating at 250 °C for 5 hours until it becomes powder. The heated powder was put into 100 mL of 1 M NaOH solution and stirred for 1 hour at 90 °C to remove the mesoporous silica mold. The synthesized product was washed using distilled water and dried again at 60 °C overnight. The resulting dry solid is a G-Ni-Zn photocatalyst. The same steps were repeated for the synthesis of G-Ni-Cu-Zn photocatalyst, with variations in photocatalyst composition as listed in the Table 1.

2.5 Photocatalytic Activity Evaluation

The photocatalytic performance of the synthesized materials was assessed via the degradation of methylene blue (MB) under UV light. In a typical test, 50 mg of catalyst was added to 0.2 L of MB solution (10 mg/L). The suspension was stirred in the dark for 120 min to establish adsorption – desorption equilibrium. Photodegradation was then initiated under UV irradiation (λ = 365 nm) for 90 min. Aliquots were taken at 10 min intervals, filtered immediately, and the residual MB concentration was analyzed using a UV–Vis spectrophotometer at λ_{max} = 664 nm.

3. Result and Discussion

Figure 1 shows the diffractograms of G-Ni-Zn and G-Ni-Cu-Zn photocatalysts. Based on the results of the diffractogram, there is uniformity of the amorphous phase because it has a wide curve. The appearance of the diffractogram on G-Ni-Cu-Zn is at a 2θ angle of about 20.86°, while G-Ni-Zn

Table 1. Compositional ratios of metal precursors and SPG-20 for catalyst preparation

Catalyst	$Ni(NO_3)_2.6H_2O$ (g)	$Cu(NO_3)_2.6H_2O$ (g)	$Zn(NO_3)_2.6H_2O$ (g)	SPG-20 (g)
G-Ni-Zn	3.32	-	1.50	1.25
G-Ni-Cu-Zn	2.48	0.67	1.14	1.25

does not show a specific peak but still contains SPG-20 at a 2θ peak of 26.64°. The non-specific peaks in this diffractogram occur due to the presence of NiO and ZnO that enter the pores of SPG-20 resulting in restructuring that changes the amorphous diffraction pattern, and if these metals diffuse into the silica network, new bonds can be formed between metals and silica that disturb the initial amorphous structure of SPG-20, causing the diffractogram pattern to become flat [25]. SPG-20, which is one type of amorphous mesoporous silica, generally shows a characteristic wide diffraction peak in the 2θ angle range of about 20° to 40° which corresponds to JCPDS No. 00-046-1045 [26]. This peak is not sharp as the crystalline phase, but rather forms a broad curve that characterizes the amorphous structure.

In XRD analysis, the presence of SPG-20 in the angle range indicates that there is still a residual mesoporous silica mold that has not completely disappeared despite the washing and calcination process. The cause of the mesoporous silica mold has not been completely separated, namely too short a soaking time with NaOH, which is only 1 hour and a less strong NaOH concentration of only 1 M [27].

The Figure 1 presents the X-ray Diffraction patterns of two photocatalyst composites. The differences observed in the diffraction patterns reflect variations in crystallinity and phase composition, which are expected to influence their photocatalytic performance in methylene blue degradation. Both samples exhibit diffraction peaks corresponding to NiO and ZnO phases at specific 2θ positions. In the G-Ni-Cu-Zn sample, additional peaks indicate the presence of CuO, confirming the successful incorporation of copper oxide. These metal oxide phases play an important role in enhancing photocatalytic efficiency by facilitating effective electron-hole separation and improving light absorption across a broader range of the spectrum. Moreover, the presence of broad diffraction features at certain angles indicates an amorphous mesoporous silica structure, which contributes to a high surface area and strong dye adsorption capacity. This enhances the interaction between methylene blue molecules and the active photocatalytic sites. The XRD pattern of G-Ni-Cu-Zn shows sharper and more intense peaks compared to G-Ni-Zn, indicating a higher degree of crystallinity. This improved crystallinity, together with the synergistic effects of NiO, ZnO, and CuO, is expected to enhance photocatalytic performance by promoting better charge mobility, reducing electron-hole recombination, and increasing the availability of active sites for photodegradation reactions.

Figure 2 shows the N_2 adsorption-desorption graph of G-Ni-Zn which tends to approach type II with a slightly less sharp curve [28]. This indicates that the pore structure of G-Ni-Zn is not completely dominated by mesopores, and there is also a contribution of macropores or the influence of a less organized bulk structure. The fit of the data to the BET linear model is also lower as indicated by the R^2 (COD) value of 0.89 and adjusted R^2 of 0.88, which is much lower than the previous two samples. This indicates that the specific surface of G-Ni-Zn is lower or less ideal in terms of monolayer adsorption of N_2. This impacts the photocatalytic activity as a lower specific surface area will reduce the number of active sites available for the photodegradation process. In addition, a non-optimal pore structure may hinder the diffusion of methylene blue molecules towards the active surface, thus lowering the efficiency of the interaction between the catalyst and the pollutant.

Table 2 shows that G-Ni-Zn has a relatively low photocatalyst performance due to its physical characteristics that are less supportive of the photodegradation process. The very small pore diameter (2.39 nm) and very low total pore volume

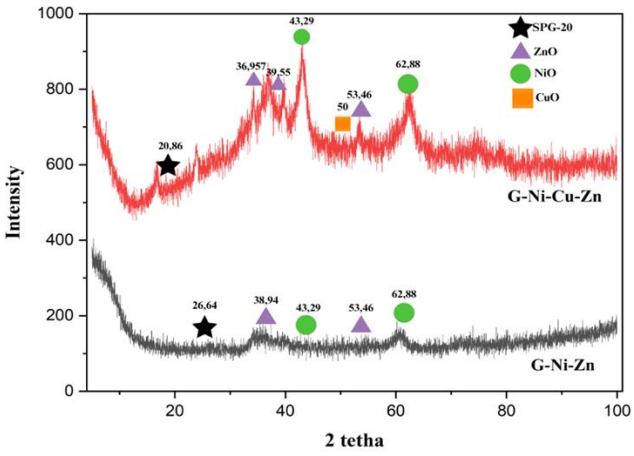

Figure 1. XRD analysis of sulfonated mesoporous silica and its composites with NiO, CuO and ZnO.

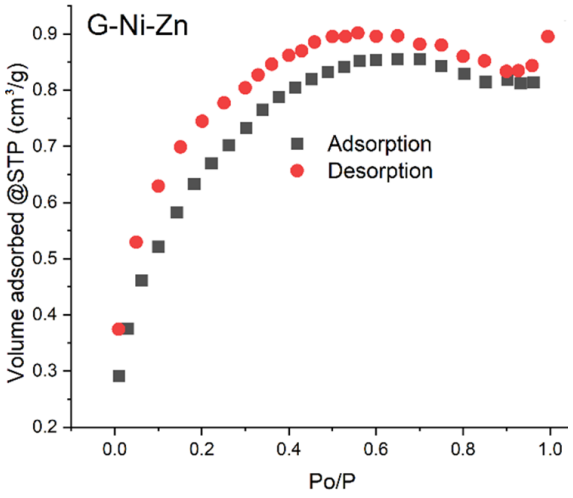

Figure 2. Isoterm adsorption desorption G-Ni-Zn composites.

(0.0014 cm^3/g) indicate that this material has limited space for the diffusion of methylene blue molecules towards the active site. In addition, the very low specific surface area based on BET and BJH analysis (only 2.32 m^2/g and 0.21 m^2/g, respectively) indicates a very limited number of active sites on the surface of the material. This condition is caused by particle agglomeration during the synthesis process or uneven distribution of active metals, thus covering most of the pores or active surfaces. As a result, the ability of the material to absorb light, separate electron-hole pairs, as well as facilitate the degradation of target molecules is very limited.

Figure 3 and Table 3 show the band gap energy of G-Ni-Zn and G-Ni-Cu-Zn photocatalysts analyzed by Kubelka Munk. The results of UV-DRS analysis of the G-Ni-Zn photocatalyst obtained a band gap energy value of 2.129 eV. This value is lower than the theoretical band gap of each constituent component, namely NiO (3.4 - 4.0 eV) and ZnO (3.37 eV). The decrease in band gap energy is due to the charge transfer between semiconductors (NiO and ZnO) and the contribution of SPG-20 which can cause the emergence of energy levels between the conduction band and valence band (defect states) or changes in the energy band structure. These defect states cause electrons to not need to jump directly from the valence band to the conduction band, but instead transition via the intermediate energy levels created by defects, thereby making the experimentally observed band gap appear narrower [20]. The band gap energy of the G-Ni-Cu-Zn sample is 3.164 eV. This value is below the theoretical band gap of NiO (3.4-4 eV) and ZnO (3.37 eV), but higher than CuO (1.2-1.4 eV). The decrease in band gap value indicates the interaction between metal oxides that form heterostructures, thus modifying the energy band structure of the material. This narrower band gap value is advantageous in a photocatalytic context because it allows the material to absorb light at longer wavelengths, including in the visible light spectrum. As such, G-Ni-Cu-Zn is potentially more active under broader illumination, as well as supporting more efficient charge transfer and inhibiting electron-hole pair recombination.

Figure 4 shows the SEM imaging of the G-Ni-Zn and G-Ni-Cu-Zn photocatalysts. The G-Ni-Zn samples show particle morphology that tends to be flat plate-shaped and irregular with a relatively smooth surface. There appears to be plate-shaped particle fragmentation with some smaller particles enveloping or attached to larger particles, and agglomeration is also present, although to a lesser extent. Flat plate shapes that tend to be dense and smooth can limit the number of active sites available for photocatalytic reactions, as well as reduce the ability to absorb light and transfer charge efficiently. The presence of small attached particle structures can slightly increase the active area, but if the distribution is uneven or not porous enough, the efficiency

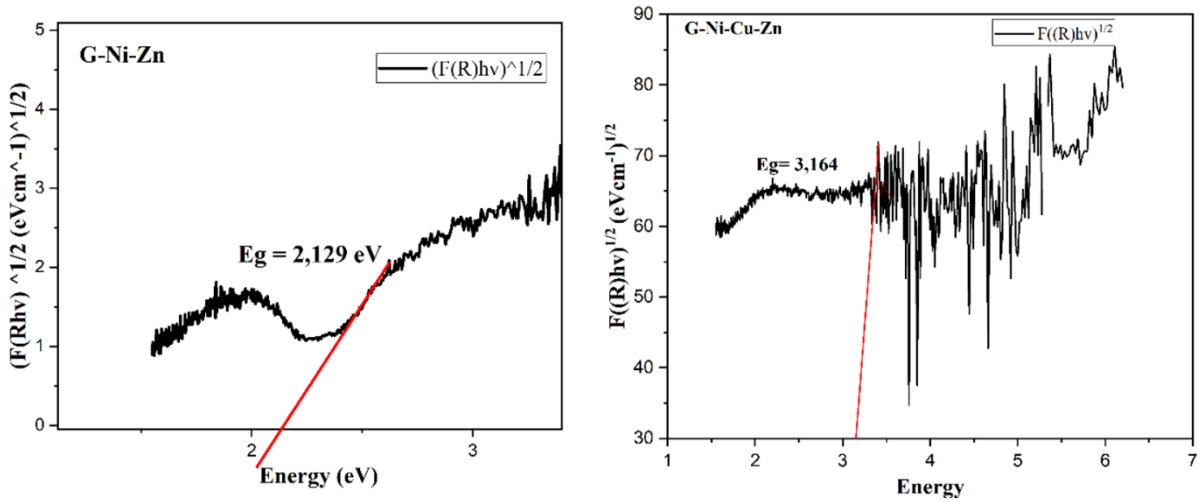

Figure 3. Band gap energy graphs of G-Ni-Zn and G-Ni-Cu-Zn photocatalysts.

Table 2. BET analysis results on G-Ni-Zn photocatalysts.

Catalyst	Pore Diameter (nm)	Total Pore Volume (cm^2/g)	BET Surface Area (m^2)	BJH Surface Area (m^2/g)
G-Cu-Ni	4.39	0.08	77.35	33.74
G-Cu-Zn	15.73	0.16	40.45	44.84
G-Ni-Zn	2.39	0.0014	2.32	0.21

remains limited. Thus, although G-Ni-Zn shows a relatively more organized morphology, its physical characteristics do not fully support the optimal enhancement of photocatalytic activity.

The G-Ni-Cu-Zn photocatalyst exhibits an irregular particle morphology characterized by a combination of flat plate-like structures and granular shapes. Some particles appear as thin, flat layers that develop into stepped arrangements, suggesting the presence of crystalline phases. The particles are distributed in a powder form with a compact yet not fully dense arrangement, accompanied by a moderate degree of agglomeration. Despite this agglomeration, the relatively loose packing of the particles facilitates light penetration and charge transfer. The visible pores in Figure 4 are mainly mesoporous voids formed between the stacked plate-like layers and intergranular spaces, which provide accessible pathways for reactants and enhance photocatalytic efficiency. Such a morphological combination, along with the pore distribution, provides an enlarged reactive surface area, enhances electron–hole mobility, and prolongs the lifetime of charge carriers, thereby contributing positively to the improvement of photocatalytic activity and pollutant degradation efficiency.

Figure 5 shows the average particle diameters of the G-Ni-Zn and G-Ni-Cu-Zn samples of 0.46 µm and 26 nm respectively showing a significant size difference, where G-Ni-Cu-Zn has much smaller particles. Smaller particle size, as in G-Ni-Cu-Zn is very advantageous in photocatalytic applications as it results in a larger surface area, thus providing more active sites for reaction. In addition, nanoparticles can shorten the diffusion distance of charges, which ultimately reduces the possibility of charge recombination and increases the efficiency of charge transfer to the reactive surface. On the contrary, the relatively large particle size of G-Ni-Zn limits the surface area and active sites, and may slow down the charge transfer, which results in the decrease of photocatalytic efficiency. Therefore, the nano-sized particles in G-Ni-Cu-Zn contribute greatly to the improvement of photocatalytic performance compared to G-Ni-Zn.

The photocatalyst test on methylene blue photodegradation aims to obtain the most effective type of photocatalyst in producing -OH radicals and contact between -OH radicals with methylene blue substrate in the degradation process under dark conditions [23]. This photodegradation process is carried out using UV-Visible. The use of UV-Visible in the photodegradation process is based on the working principle of photocatalysts that require light energy to activate electrons in semiconductor materials. When G-Ni-Zn and G-Ni-Cu-Zn

Table 3. Band gap of G-Ni-Zn.

Sample	Experimental Band Gap (eV)	Theoretical Band Gap (E_v)
G-Ni-Zn	2.129	NiO = 3.4 – 4 eV [29] ZnO = 3.37 eV [30]
G-Ni-Cu-Zn	3.164	NiO = 3.4 – 4 eV [29] CuO = 1.2 – 1.4 eV [31] ZnO = 3.37 eV [30]

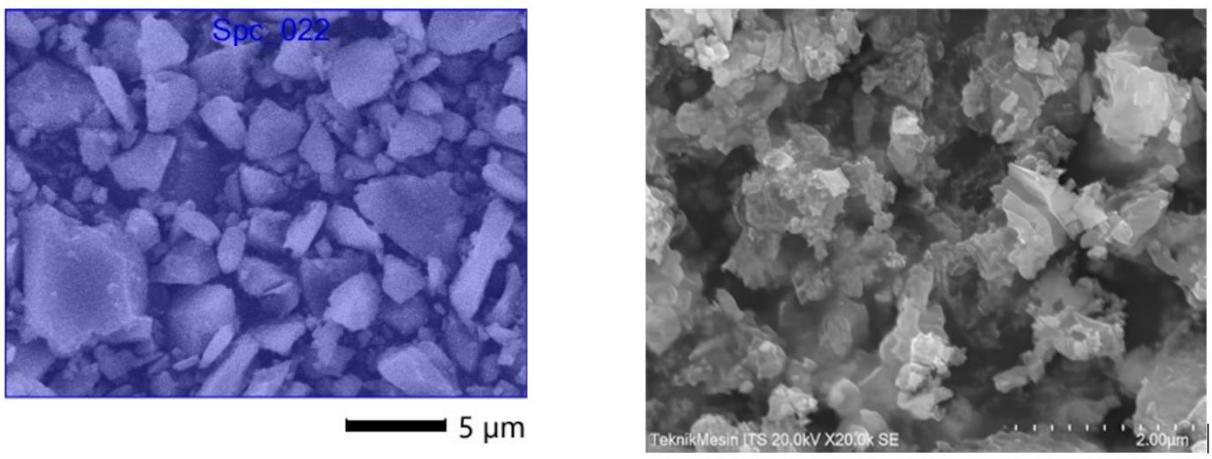

(a) (b)

Figure 4. Pore size distribution of : a. G-Ni-Zn. b. G-Ni-Cu-Zn.

photocatalysts are exposed to light with sufficient energy, especially from the ultraviolet (UV) spectrum or visible light, electrons in the valence band will be excited to the conduction band and then leave holes in the valence band. This event produces a highly reactive electron-hole pair (e^-/h^+). These electrons and holes contribute to the formation of reactive oxygen species (ROS), such as hydroxyl radicals ($\cdot OH$) and superoxide anions ($O_2^{\cdot -}$), which are highly reactive and capable of degrading complex organic compounds into smaller molecules, and eventually mineralizing them into CO_2 and H_2O [32].

Figure 6 shows that the degradation trend of methylene blue dye tends to increase. Theoretically, photodegradation efficiency increases over time because the longer the contact time between methylene blue with photocatalyst and UV light, the more pollutant molecules are degraded [33]. In the dark adsorption process for 10 minutes, the physical adsorption process tends to increase from the 0th minute to the 10th minute due to the shaker process. The dark adsorption process is carried out before the uv light irradiation process is carried out with the aim of homogenizing the solution and achieving equilibrium so that when the methylene blue solution is irradiated it is degraded more quickly. This is because some of the methylene blue dye molecules have been trapped on the surface of the nanoparticles so as to facilitate the passage of UV light to the hole in the photocatalyst [12].

In irradiation during the 15th minute to the 120th minute there was an increase in degradation. This is because the longer the irradiation process, the more pollutant molecules are degraded. The success of the degradation process is indicated by the reduced concentration of methylene blue dye at the 0th minute of irradiation time until the time of increasing irradiation time. In addition, with the addition of irradiation time, the photon energy absorbed by photocatalysts, especially on mesoporous silica catalysts that are embedded with NiO, CuO, and ZnO metal oxides, is increasing so that it is easy to degrade methylene blue dye. The process of embedding with metal oxides can reduce the energy gap (band gap) on the catalyst and increase the charge transfer on the catalyst surface [34].

The ZnO:NiO:CuO system reported by Ishaque *et al.* [36] achieved 98% efficiency in 90 minutes under sunlight, which is higher than our result. However, their system used direct sunlight irradiation and different synthesis conditions. Our hard template approach using gelatin-derived mesoporous silica provides structural advantages in terms of controlled porosity and metal oxide dispersion.

Table 4 shows the maximum degradation efficiency by G-Ni-Zn and G-Ni-Cu-Zn photocatalysts. The photodegradation of methylene blue by G-Ni-Zn photocatalyst shows a relatively low to moderate photodegradation efficiency with a maximum value of about 30.03% at the 120th minute. When compared, the

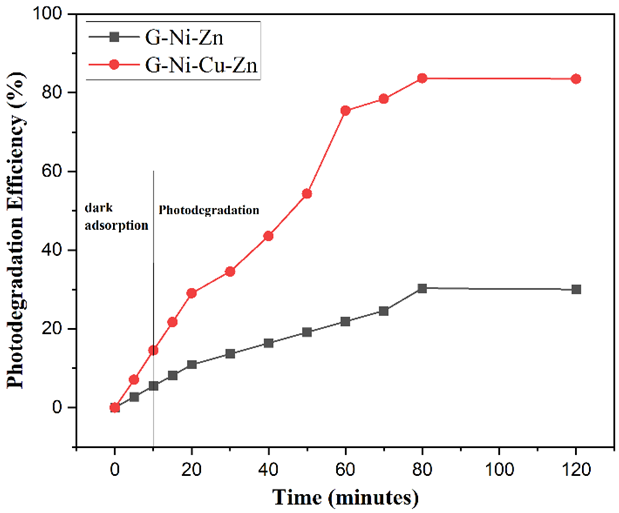

Figure 6. Effect of catalyst modification on MB photodegradation efficiency under UV light.

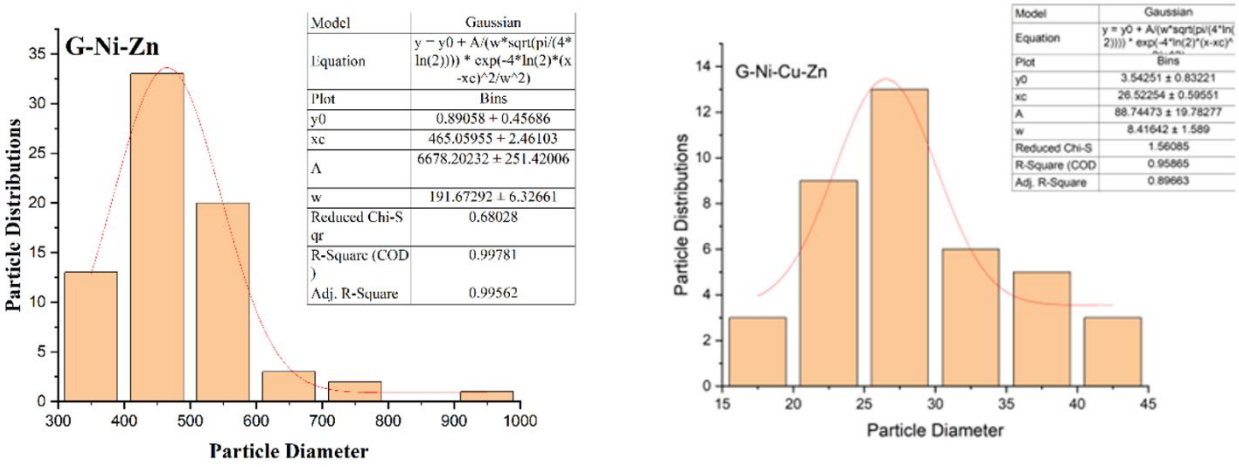

Figure 5. SEM agglomerate size by SEM for all sample.

performance of this photocatalyst is far below G-Cu-Ni which is able to achieve an efficiency of almost 80%, and still lower than G-Cu-Zn which reaches about 51%. The increase in efficiency of G-Ni-Zn was so slow that until the 50th minute, the efficiency only reached around 19%. This shows that its photocatalytic activity is not very responsive to light irradiation in a short time. This could be because the combination of Ni-Zn without Cu is not effective enough in generating and maintaining the stability of electron-hole pairs. Although Ni can help suppress recombination, the absence of Cu as a charge transfer bridge can cause obstacles in electron mobility towards the active surface [41]. In addition, Zn which has a large band gap also tends to be less responsive to visible light, limiting the photocatalyst's ability to utilize light energy efficiently.

Methylene blue (MB) photodegradation efficiency using G-Ni-Cu-Zn photocatalyst showed a significant increase with time. In the initial stage (0-10 min), there was an adsorption process under dark conditions which indicated the initial ability of the catalyst to attract MB molecules to the surface. Once irradiation starts (photodegradation phase), the degradation efficiency increases sharply, especially in the first 60 min, indicating high photocatalytic activity. The curve then starts to slope and reaches a maximum efficiency of 83.67% at 90th to 120th minutes, indicating that most of the MB molecules have been degraded and the system starts to reach a saturated state. This high performance indicates that G-Ni-Cu-Zn has an excellent ability to absorb light and generate effective electron-hole pairs to degrade organic pollutants such as MB.

4. Conclusion

The use of Ni-Cu-Zn combination photocatalyst modified with mesoporous silica gelatin (mSG) is very effective in the photodegradation process of methylene blue (MB) dye waste. The test results showed that the G-Ni-Cu-Zn photocatalyst achieved a maximum degradation efficiency of 83.67% within 120 minutes, much higher than that of G-Ni-Zn which only reached 30.31%. This increase in efficiency can be attributed to the ability of G-Ni-Cu-Zn to absorb light and generate effective electron-hole pairs, which are crucial in the degradation process of organic compounds. In addition, the combination of Ni, Cu, and Zn metals provides a synergy that increases charge mobility and reduces recombination, thus accelerating the degradation process. This research confirms the importance of developing efficient and environmentally friendly photocatalysts to address the problem of textile waste pollution, particularly in the context of a growing industry

Acknowledgment

This work was financially supported by Universitas Sebelas Maret (UNS) through the 2025 Applied Leading Research Grant Scheme A (Penelitian Unggulan Terapan A, PUTA UNS), under contract number 369/UN27.22/PT.01.03/2025. The authors sincerely acknowledge the institutional support and funding provided by UNS, which played a crucial role in enabling the successful execution of this research.

CRedit Author Statement

Author Contributions: M. Ulfa: Conceptualization, Investigation, Methodology, Formal Analysis, Resources, Data Curation, Validation,Writing – Original Draft, Writing – Review & Editing, Supervision,; S. Lestari: Project Administration Methodology, Formal Analysis, Data Curation, Writing – Original Draft Preparation, Writing – Review & Editing, Data Curation. All authors have read and agreed to the published version of the manuscript.

Table 4. Maximum degradation efficiency values by G-Ni-Zn and G-Ni-Cu-Zn.

Photocatalyst	Maximum degradation efficiency (%)	Time (min)	Conditions	Reference
G-Ni-Zn	30.31	120	UV light, 10 mg/L MB	This work
G-Ni-Cu-Zn	83.66	120	UV light, 10 mg/L MB	This work
NiO/ZnO composite	97.0	175	UV light, 7 mg/L MB	[6]
CuO/ZnO (4:6 ratio)	93.0	60	Green LED, 5 mg/L MB	[35]
ZnO:NiO:CuO (1:1:2)	98.0	90	Sunlight, 10 mg/L MB	[36]
TiO_2/mesoporous silica	95.81	90	UV light, 10 mg/L MB	[37]
Fe_2O_3/SPG_{20}–SO_3H	92.14	120	UV light, 10 mg/L MB	[38]
ZnO/NiO nanocomposite	89.8	175	UV light, 7 mg/L MB	[39]
Mn_3O_4@ZnO hybrid	94.59	70	UV light, MB solution	[40]

References

[1] Prasetyoko, D., Sholeha, N.A., Subagyo, R., Ulfa, M., Bahruji, H., Holilah, H., Pradipta, M.F., Jalil, A.A. (2023). Mesoporous ZnO nanoparticles using gelatin - Pluronic F127 as a double colloidal system for methylene blue photodegradation. *Korean Journal of Chemical Engineering,* 40(1), 112–123. DOI: 10.1007/s11814-022-1224-y.

[2] Ulfa, M., Nina, Pangestuti, I., Holilah, Bahruji, H., Rilda, Y., Alias, S.H., Nur, H. (2024). Enhancing photocatalytic activity of Fe2O3/TiO2 with gelatin: A fuzzy logic analysis of mesoporosity and iron loading. *South African Journal of Chemical Engineering*, 50(August), 245–260. DOI: 10.1016/j.sajce.2024.08.011.

[3] de Souza, C.C., de Souza, L.Z.M., Yılmaz, M., de Oliveira, M.A., da Silva Bezerra, A.C., da Silva, E.F., Dumont, M.R., Machado, A.R.T. (2022). Activated carbon of Coriandrum sativum for adsorption of methylene blue: Equilibrium and kinetic modeling. *Cleaner Materials*, 3 (October 2021). DOI: 10.1016/j.clema.2022.100052.

[4] Alkayal, N.S., Altowairki, H., Alosaimi, A.M., Hussein, M.A. (2022). Network template-based cross-linked Poly(methyl methacrylate)/tin(IV) oxide nanocomposites for the photocatalytic degradation of MB under UV irradiation. *Journal of Materials Research and Technology*, 18, 2721–2734. DOI: 10.1016/j.jmrt.2022.03.133.

[5] Wei, J.Q., Chen, X.J., Wang, P.F., Han, Y.B., Xu, J.C., Hong, B., Jin, H.X., Jin, D.F., Peng, X.L., Li, J., Yang, Y.T., Ge, H.L., Wang, X.Q. (2018). High surface area TiO2/SBA-15 nanocomposites: Synthesis, microstructure and adsorption-enhanced photocatalysis. *Chemical Physics*, 510, 47–53. DOI: 10.1016/j.chemphys.2018.05.012.

[6] Weldekirstos, H.D., Habtewold, B., Kabtamu, D.M. (2022). Surfactant-Assisted Synthesis of NiO-ZnO and NiO-CuO Nanocomposites for Enhanced Photocatalytic Degradation of Methylene Blue Under UV Light Irradiation. *Frontiers in Materials*, 9(April), 1–10. DOI: 10.3389/fmats.2022.832439.

[7] Dymerska, A., Zielińska, B., Sielicki, K., Chen, X., Mijowska, E. (2022). Porous silica matrix as an efficient strategy to boosted photocatalytic performance of titania/carbon composite. *Diamond and Related Materials*, 125(February) DOI: 10.1016/j.diamond.2022.109027.

[8] Li, S., Cui, Y., Wen, M., Ji, G. (2023). Toxic Effects of Methylene Blue on the Growth, Reproduction and Physiology of Daphnia magna. *Toxics*, 11(7) DOI: 10.3390/toxics11070594.

[9] Oladoye, P.O., Kadhom, M., Khan, I., Hama Aziz, K.H., Alli, Y.A. (2024). Advancements in adsorption and photodegradation technologies for Rhodamine B dye wastewater treatment: fundamentals, applications, and future directions. *Green Chemical Engineering*, 5(4), 440–460. DOI: 10.1016/j.gce.2023.12.004.

[10] Tongon, W., Chawengkijwanich, C., Chiarakorn, S. (2014). Visible light responsive Ag/TiO2/MCM-41 nanocomposite films synthesized by a microwave assisted sol–gel technique. *Superlattices and Microstructures*, 69, 108–121. DOI: 10.1016/j.spmi.2014.02.003.

[11] Sahu, D., Pervez, S., Karbhal, I., Tamrakar, A., Mishra, A., Verma, S.R., Deb, M.K., Ghosh, K.K., Pervez, Y.F., Shrivas, K., Satnami, M.L. (2024). Applications of different adsorbent materials for the removal of organic and inorganic contaminants from water and wastewater – A review. *Desalination and Water Treatment*, 317(February), 100253. DOI: 10.1016/j.dwt.2024.100253.

[12] Khan, S., Noor, T., Iqbal, N., Yaqoob, L. (2024). Photocatalytic Dye Degradation from Textile Wastewater: A Review. *ACS Omega*, 9(20), 21751–21767. DOI: 10.1021/acsomega.4c00887.

[13] Sun, Y., Zhang, W., Li, Q., Liu, H., Wang, X. (2023). Preparations and applications of zinc oxide based photocatalytic materials. *Advanced Sensor and Energy Materials*, 2(3), 100069. DOI: 10.1016/j.asems.2023.100069.

[14] Zhang, Y., Tang, Z.-R., Fu, X., Xu, Y.-J. (2010). TiO_2-Graphene Nanocomposites for Gas-Phase Photocatalytic Degradation of Volatile Aromatic Pollutant: Is TiO_2-Graphene Truly Different from Other TiO_2-Carbon Composite Materials? *ACS Nano*, 4(12), 7303–7314. DOI: 10.1021/nn1024219.

[15] Li, J., Han, L., Zhang, T., Qu, C., Yu, T., Yang, B. (2022). Removal of Methylene Blue by Metal Oxides Supported by Oily Sludge Pyrolysis Residues. *Applied Sciences (Switzerland)*, 12(9). DOI: 10.3390/app12094725.

[16] Albiss, B., Abu-Dalo, M. (2021). Photocatalytic degradation of methylene blue using zinc oxide nanorods grown on activated carbon fibers. *Sustainability (Switzerland)*, 13(9). DOI: 10.3390/su13094729.

[17] Kanakaraju, D., bin Ya, M.H., Lim, Y.C., Pace, A. (2020). Combined Adsorption/Photocatalytic dye removal by copper-titania-fly ash composite. *Surfaces and Interfaces*, 19(January), 100534. DOI: 10.1016/j.surfin.2020.100534.

[18] Soleimani-Gorgani, A., Al-Hazmi, H.E., Esmaeili, A., Habibzadeh, S. (2023). Screen-printed Sn-doped TiO2 nanoparticles for photocatalytic dye removal from wastewater: A technological perspective. *Environmental Research*, 237(P2), 117079. DOI: 10.1016/j.envres.2023.117079.

[19] Dhiman, P., Rana, G., Dawi, E.A., Kumar, A., Sharma, G., Kumar, A., Sharma, J. (2023). Tuning the Photocatalytic Performance of Ni-Zn Ferrite Catalyst Using Nd Doping for Solar Light-Driven Catalytic Degradation of Methylene Blue. *Water (Switzerland)*, 15(1). DOI: 10.3390/w15010187.

[20] Xu, L., Su, J., Zheng, G., Zhang, L. (2019). Enhanced photocatalytic performance of porous ZnO thin films by CuO nanoparticles surface modification. *Materials Science and Engineering: B*, 248(January) DOI: 10.1016/j.mseb.2019.114405.

[21] Nawaz, A., Farhan, A., Maqbool, F., Ahmad, H., Qayyum, W., Ghazy, E., Rahdar, A., Díez-Pascual, A.M., Fathi-karkan, S. (2024). Zinc oxide nanoparticles: Pathways to micropollutant adsorption, dye removal, and antibacterial actions - A study of mechanisms, challenges, and future prospects. *Journal of Molecular Structure*, 1312(P1), 138545. DOI: 10.1016/j.molstruc.2024.138545.

[22] Costa, J.A.S., De Jesus, R.A., Santos, D.O., Neris, J.B., Figueiredo, R.T., Paranhos, C.M. (2021). Synthesis, functionalization, and environmental application of silica-based mesoporous materials of the M41S and SBA-n families: A review. *Journal of Environmental Chemical Engineering*, 9(3). DOI: 10.1016/j.jece.2021.105259.

[23] Ulfa, M., Anggreani, C.N., Mulyani, B., Sholeha, N.A. (2024). Hexagonal TiO2/SiO2 Porous Microplates for Methylene Blue Photodegradation. *Bulletin of Chemical Reaction Engineering & Catalysis*, 19(1), 149–159. DOI: 10.9767/bcrec.20120.

[24] Kausar, S., Yousaf, M., Mir, S., Awwad, N.S., Alturaifi, H.A., Riaz, F. (2024). Mesoporous Materials: Synthesis and electrochemical applications. *Electrochemistry Communications*, 169 (October), 107836. DOI: 10.1016/j.elecom.2024.107836.

[25] Bastakoti, B.P., Kuila, D., Salomon, C., Konarova, M., Eguchi, M., Na, J., Yamauchi, Y. (2021). Metal-incorporated mesoporous oxides: Synthesis and applications. *Journal of Hazardous Materials*, 401(June 2020), 123348. DOI: 10.1016/j.jhazmat.2020.123348.

[26] Klinkaewnarong, J., Utara, S. (2018). Ultrasonic-assisted conversion of limestone into needle-like hydroxyapatite nanoparticles. *Ultrasonics Sonochemistry*, 46(March), 18–25. DOI: 10.1016/j.ultsonch.2018.04.002.

[27] Ghaedi, H., Zhao, M. (2022). Review on Template Removal Techniques for Synthesis of Mesoporous Silica Materials. *Energy and Fuels*, 36 (5), 2424–2446. DOI: 10.1021/acs.energyfuels.1c04435.

[28] Barczak, M. (2018). Template removal from mesoporous silicas using different methods as a tool for adjusting their properties. *New Journal of Chemistry*, 42(6), 4182–4191. DOI: 10.1039/c7nj04642a.

[29] Yousaf, S., Zulfiqar, S., Shahi, M.N., Warsi, M.F., Al-Khalli, N.F., Aly Aboud, M.F., Shakir, I. (2020). Tuning the structural, optical and electrical properties of NiO nanoparticles prepared by wet chemical route. *Ceramics International*, 46(3), 3750–3758. DOI: 10.1016/j.ceramint.2019.10.097.

[30] Hasnidawani, J.N., Azlina, H.N., Norita, H., Bonnia, N.N., Ratim, S., Ali, E.S. (2016). Synthesis of ZnO Nanostructures Using Sol-Gel Method. *Procedia Chemistry*, 19, 211–216. DOI: 10.1016/j.proche.2016.03.095.

[31] Gokul, G., Thirumaran, S. (2025). Structural, morphological, optical and photocatalytic properties of copper oxide nanoparticles prepared by thermal decomposition of bis(N-dodecyl-N-(4-fluorobenzyl)dithiocarbamato-S,S')copper(II). *Journal of Molecular Structure*, 1333 (January), 141686. DOI: 10.1016/j.molstruc.2025.141686.

[32] Koe, W.S., Lee, J.W., Chong, W.C. (2019). An overview of photocatalytic degradation: photocatalysts, mechanisms, and development of photocatalytic membrane. *Colloid and Interface Science Journal*, 44. DOI: 10.1007/s11356-019-07193-5.

[33] Naffeti, M., Zaïbi, M.A., Nefzi, C., García-Arias, A.V., Chtourou, R., Postigo, P.A. (2023). Highly efficient photodegradation of methylene blue by a composite photocatalyst of bismuth nanoparticles on silicon nanowires. *Environmental Technology and Innovation*, 30. DOI: 10.1016/j.eti.2023.103133.

[34] Raizada, P., Soni, V., Kumar, A., Singh, P., Parwaz Khan, A.A., Asiri, A.M., Thakur, V.K., Nguyen, V.H. (2021). Surface defect engineering of metal oxides photocatalyst for energy application and water treatment. *Journal of Materiomics*, 7(2), 388–418. DOI: 10.1016/j.jmat.2020.10.009.

[35] Dien, N.D., Thu Ha, P.T., Vu, X.H., Trang, T.T., Thanh Giang, T.D., Dung, N.T. (2023). Developing efficient CuO nanoplate/ZnO nanoparticle hybrid photocatalysts for methylene blue degradation under visible light. *RSC Advances*, 13(35), 24505–24518. DOI: 10.1039/d3ra03791f.

[36] Ishaque, M.Z., Zaman, Y., Arif, A., Siddique, A.B., Shahzad, M., Ali, D., Aslam, M., Zaman, H., Faizan, M. (2023). Fabrication of ternary metal oxide (ZnO:NiO:CuO) nanocomposite heterojunctions for enhanced photocatalytic and antibacterial applications. *RSC Advances*, 13(44), 30838–30854. DOI: 10.1039/d3ra05170f.

[37] Ulfa, M., Nur, C., Amalia, N. (2023). Fine-tuning mesoporous silica properties by a dual-template ratio as TiO2 support for dye photodegradation booster. *Heliyon*, 9(6), e16275. DOI: 10.1016/j.heliyon.2023.e16275.

[38] Ulfa, M., Salsabila, P.R., Saputro, A.N.C., Nurhayati, N.D. (2025). Methylene Blue Degradation with Sulfonated SPG20 Silica-Fe2O3 Hybrid Photocatalysts. *Bulletin of Chemical Reaction Engineering & Catalysis*, 20 (3), 441–457. DOI: 10.9767/bcrec.20380.

[39] Iasya, Y.K.A.A., Khoerunnisa, F., Dewi, S.S., Putri, R.A., Nurhayati, M., Arrozi, U.S.F., Permana, Y., Handayani, M., Astuti, W.D., Da, O.W., Irnanda, I. (2025). Synergetic effect of ZnO/NiO nanocomposite on the enhancement of photocatalytic degradation efficiency of dyes molecules. *Communications in Science and Technology*, 10(1), 1–9. DOI: 10.21924/cst.10.1.2025.1583.

[40] Shaikh, B., Bhatti, M.A., Shah, A.A., Tahira, A., Shah, A.K., Usto, A., Aftab, U., Bukhari, S.I., Alshehri, S., Shah Bukhari, S.N.U., Tonezzer, M., Vigolo, B., Ibhupoto, Z.H. (2022). Mn3O4@ZnO Hybrid Material: An Excellent Photocatalyst for the Degradation of Synthetic Dyes including Methylene Blue, Methyl Orange and Malachite Green. *Nanomaterials*, 12 (21), 1–16. DOI: 10.3390/nano12213754.

[41] Chen, S., Farzinpour, F., Kornienko, N. (2025). Dynamic active sites behind Cu-based electrocatalysts: Original or restructuring-induced catalytic activity. *Chem*, 11(8), 102575. DOI: 10.1016/j.chempr.2025.102575.